Catalysis Letters 55 (1998) 113–120

Diffusional characteristics of substituted anilines in various zeolites as predicted by molecular modeling methods

P. Bharathi, R.C. Deka, S. Sivasanker and R. Vetrivel *

Catalysis Division, National Chemical Laboratory, Pune 411008, India

Received 27 May 1998; accepted 29 August 1998

Energy minimization methodology is used to study the interaction of substituted aniline molecules in various zeolites. The adsorption sites inside the zeolite channels and the diffusion characteristics of acylated products of 4-aminophenol are analyzed in detail. The selective formation of 4-hydroxyacetanilide, which is a pharmaceutically important compound, over various zeolites is studied. Three large-pore zeolites having 12-MR channel systems are selected: (i) zeolite-L with barrel-shaped cages, (ii) mazzite with circular pores and (iii) mordenite with elliptical pores and side pockets. The diffusion characteristics of the molecules are sensitive to pore architecture. The calculated diffusion energies do not indicate product selectivity in large-pore zeolites. Further, a study of diffusion inside the pores of ZSM-5, a medium-pore zeolite with 10-MR channel system, reveals that the C-acylated products have significantly larger diffusion energy barriers than the N-acylated products. The results are also useful in understanding the mode of interaction of the molecules with the zeolite framework.

Keywords: molecular modeling, substituted anilines, diffusion characteristics, shape selectivity, large- and medium-pore zeolites, aromatic acylation

1. Introduction

Aromatic acylation processes are widely used in the chemical industry for the manufacture of fine chemicals and intermediates [1]. The synthesis of several intermediates for major analgesic drugs such as paracetamol [2], Ibuprofen [1], and S-Naproxen [1] involves an aromatic acylation step. Conventionally, acid chlorides together with a stoichiometric amount of a Lewis acid, e.g., $AlCl_3$, $FeCl_3$, or $TiCl_4$, are used in the reaction [3]. The synthetic utility of this reaction is limited by the formation of a considerable amount of by-products and toxic waste. The use of Brønsted acid catalysts such as polyphosphoric acid [4] promotes side reactions such as cyclization, aromatization, and dehydration. In order to solve the above problems, some solid acid catalyzed acylations have been attempted [5]. Zeolites, which are solid acid materials, have been reported to be efficient catalysts for electrophilic substitution reactions in general [6] and acylations in particular [7]. The use of zeolites could, in principle, permit control over the chemoselectivity of the reaction through choice of their pore size, shape and acidity distribution. The application of zeolites as acylation catalysts is environmentally more acceptable due to greater selectivity and reusability.

In the present study, we have attempted to identify shape-selective zeolite catalysts suitable for the production of 4-hydroxyacetanilide (**2**) by the acylation of 4-aminophenol (**1**). The N-acylated product of 4-aminophenol (**1**), namely 4-hydroxyacetanilide (**2**), is an analgesic and antipyretic drug, paracetamol, as well as an intermediate in the manufacture of azodyes and photographic chemicals [2]. Under basic conditions, acylation is known to occur at the hydroxyl group leading to 4-aminophenylacetate (**3**), whereas under acidic conditions, the acylation takes place at the amino group, leading to (**2**). However, Lewis acid catalysts also lead to acylation of the phenyl ring leading to 4-amino-*o*-hydroxyacetophenone (**4**) and 4-amino-*m*-hydroxyacetophenone (**5**). Further, the conventional catalysts lead to multiacylated products also due to consecutive acylation. However, in the case of acidic zeolites which could lead to N-acylation, C-acylation and multiacylation could be avoided through shape selectivity effects. It was therefore decided to investigate, using molecular modeling techniques, the shape selectivity features of zeolite-L, mazzite, mordenite and ZSM-5 with different pore dimensions and topologies in the N-acylation of 4-aminophenol.

2. Methods and models

We have applied molecular modeling techniques such as molecular graphics (MG), structural fitting and force-field-based energy minimization (EM) calculations to understand the adsorption sites and diffusion characteristics of the molecules (**1**)–(**5**) shown in figure 1. The molecules were generated as MG models and their size and shapes were analyzed. The strain energy of each molecule was minimized by varying its internal geometry. The extents of the molecule in space were calculated for the energetically favorable conformation. The three largest dimensions ($a \times b \times c$) of the molecule [8] in mutually perpendicular

* To whom correspondence should be addressed.

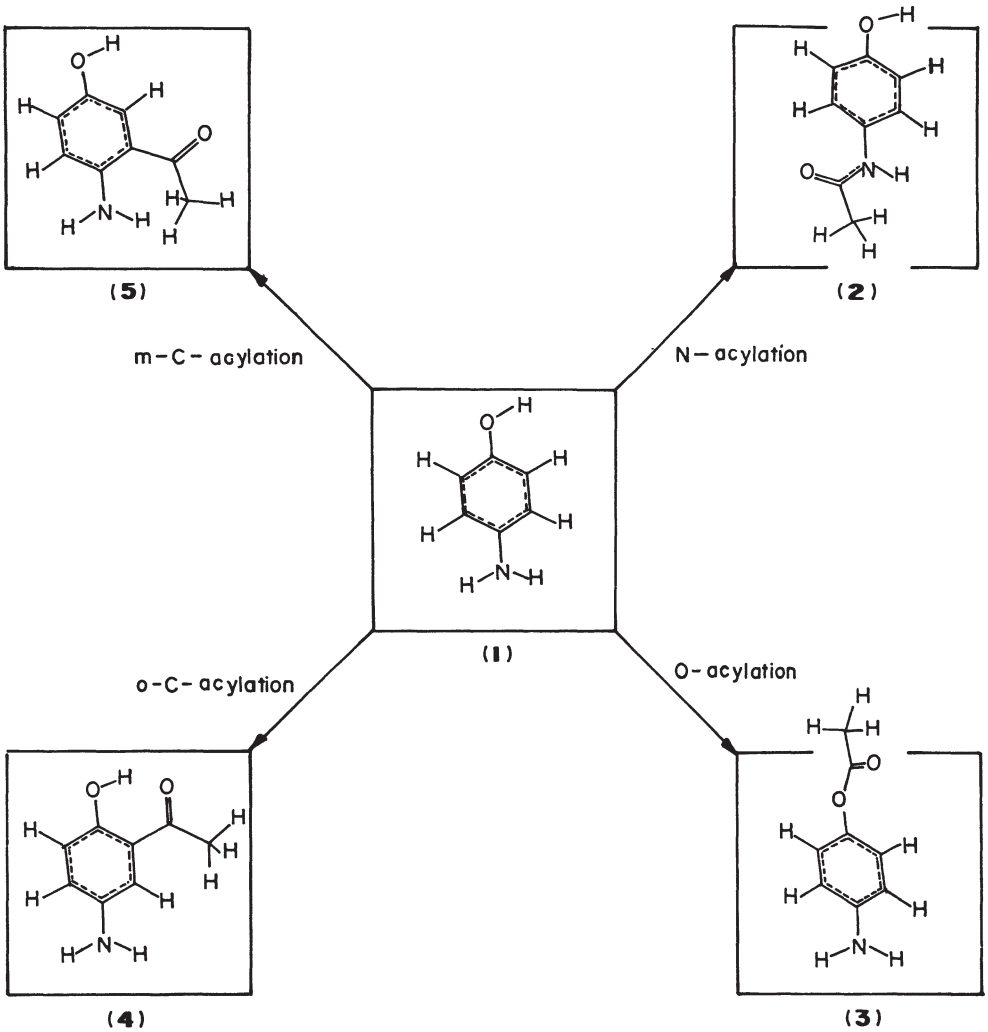

Figure 1. 3-d molecular graphics pictures of 4-aminophenol (**1**) and its possible acylated products: 4-hydroxyacetanilide (**2**), 4-aminophenylacetate (**3**), 4-amino-*o*-hydroxyacetophenone (**4**) and 4-amino-*m*-hydroxyacetophenone (**5**).

Table 1
Dimensions of different organic molecules in their minimum energy configurations.

Molecule (numbering as in figure 1)	Dimensions (Å)		
	a	*b*	*c*
1	6.09	4.35	1.82
2	8.28	5.11	4.04
3	6.82	5.78	2.63
4	6.36	6.14	2.88
5	8.84	4.59	3.00

directions are given in table 1. Various zeolite lattices were generated from the X-ray crystal structure reports. Qualitative structural fitting of the molecules inside the zeolites was studied by MG as well as by comparing the dimensions of the molecules with the pore diameters of the zeolites. Further, the chemical interaction between the zeolite host–guest molecules was studied using EM calculations. EM calculations were carried out for the custom designed diffusion paths to determine the minimum energy route for the diffusion of different molecules.

The zeolite lattices considered include three large-pore (12-MR) zeolites with different pore topologies, namely Linde type-L (LTL), mazzite (MAZ), and mordenite (MOR), and a medium-pore zeolite ZSM-5 (MFI). During the calculation of the interaction energy, the atoms in the zeolite lattice were held fixed at their crystallographically determined geometries. The simulation box contained the zeolite generated, based on its crystal structure determination. The actual dimensions of the simulation box for each zeolite are given in table 2.

The calculations were performed according to the forced diffusion procedure used by Horsley et al. [9] in the investigation of the shape selectivity properties of zeolites in the alkylation of naphthalene. Modified versions of this procedure have been used in many studies [10–12]. The sorbate molecule was forced to diffuse stepwise in regular steps of 0.2 Å along the diffusion path defined by the initial and final positions, as described in our earlier study [12]. At each point, a strong harmonic potential constrains the molecule to lie at a fixed distance from the initial position while the energetically favorable conformation and orientation are

Table 2
Crystal characteristics and the dimensions of the simulation boxes for different zeolites.

Zeolite	Symmetry	Unit cell composition	a (Å)	b (Å)	c (Å)	Average pore diameter (Å)	Number of unit cells
LTL	Hexagonal	$[SiO_2]_{36}$	18.4650	18.465	7.476	7.1	$2 \times 2 \times 8$
MAZ	Hexagonal	$[SiO_2]_{36}$	18.3920	18.392	7.646	7.4	$2 \times 2 \times 8$
MOR	Orthorhombic	$[SiO_2]_{36}$	18.0940	20.516	7.524	6.5×7.0	$1.7 \times 1.5 \times 8$
ZSM-5	Orthorhombic	$[SiO_2]_{96}$	20.0219	19.899	13.383	5.1×5.6	$3 \times 3.5 \times 2$

derived by varying their internal degrees of freedom. The forces acting between the zeolite host–guest molecule are described by the consistent valence force field (CVFF) reported by Hagler et al. [13]. The nonbonding interactions of molecules with the zeolite framework are calculated by determining the long-range forces by classical electrostatic interactions and short-range forces as described by Lennard-Jones potentials [14]. Thus, the diffusion energy profile is a graph showing the variation of interaction energy between the molecule and the zeolite framework as the molecule diffuses within the channel of the zeolite. These profiles are useful to identify the most favorable (minimum energy) and unfavorable (maximum energy) adsorption sites for the molecules inside the zeolite channels. The difference in energy between the most favorable and most unfavorable sites in the diffusion energy profile gives the diffusion energy barrier. All the molecular modeling studies were carried out in a SGI-Indigo2 workstation, using the "Solids-Docker" facility of the catalysis module software package supplied by Biosym/MSI [15].

3. Results and discussion

Shape selectivity achieved by zeolites in catalytic conversion is governed by several factors among which the relative rates of diffusion of reactants, products and intermediates play a dominant role. Information on the interactions at the molecular level is difficult to derive experimentally. However, the diffusion energy profiles calculated from interaction energies are useful to derive the diffusion energy barriers which in turn provide a good indication of the relative rates of diffusion through the pores of the zeolite. In the acylation of 4-aminophenol (**1**) there is a possibility for N-acylation (**2**), O-acylation (**3**) and C-acylation at ortho and meta positions leading to (**4**) and (**5**), as shown in figure 1. It is a necessary condition that the reactant and the product molecules involved in acylation should fit inside the pores. The molecules would prefer to enter the cages via their smallest dimensions on the basis of interaction energy criteria. A comparison of the dimensions of molecules in table 1, with those of the pore dimensions of 8-MR pore zeolites (pore diameter $\sim$4 Å) reveals that the pores of these zeolites are too small to accommodate 4-aminophenol and its acylated products. We have, therefore, chosen three large-pore (12-MR) zeolites with different pore topologies and a medium-pore zeolite (10-MR) for our studies.

3.1. Diffusion characteristics of molecules in LTL

LTL belongs to the hexagonal crystal class. The pore in zeolite-L is circular with a pore diameter of 7.1 Å. It has a structure consisting of channels along the c-direction, as shown in figure 2. The channels are built up of barrel-shaped 12-MR rings separated by 7.5 Å along the c-direction. The diameter of the barrel is the largest (12.6 Å) at the midpoint between the two 12-MR rings; there is sufficient room for the sorbate to adopt several orientations. The diffusion of the molecules along the c-direction in the 12-MR channel is considered. The initial and final points of the diffusion path are also shown in figure 2 as A and B, respectively. The diffusion calculations were carried out for all the five molecules (**1**)–(**5**) as described in the previous section. The diffusion was studied for three unit cells in the c-direction, and the results of such calculations are shown in table 3.

A typical diffusion energy profile for the molecule (**1**), as it diffuses through the 12-MR channel for two unit cells is shown in figure 2. The diffusion energy profile symmetrically repeats itself in each unit cell indicating the validity of the simulation box size, potential parameters and energy minimization calculations. The diffusion energy barriers for (**1**)–(**5**) are in the range of 6.95–15.62 kcal/mol. The interaction energy of the molecule with the framework is maximum when the molecule passes through the 12-MR ring. The interaction energy is minimum when the molecule is in the barrel-shaped cage.

In general, it is observed that when the molecules take an orientation parallel to the c-axis (during "cage-to-cage" diffusion), the interaction energy is unfavorable and when the molecules could take an orientation perpendicular to the c-axis (when inside the cage), the interaction energy is favorable. It is noticed that the diffusion energy barriers calculated for the molecules (table 3) are not in correlation with their sizes due to the very large size of the cage compared to molecules. The diffusion energy barrier was recalculated assuming diffusion of the molecules along the c-direction, with their largest dimension along the c-direction. The diffusion energy barrier values calculated using this assumption for the molecules (**1**)–(**5**) are given in parentheses. In these calculations, the energy minimization was not carried out and thus the molecule could not orient itself perpendicular to the channel axis. In this case, the energy barrier values are in correlation with their sizes. These results indicate that although LTL presents large-diameter pores for the diffusion of molecules, the molecules will still

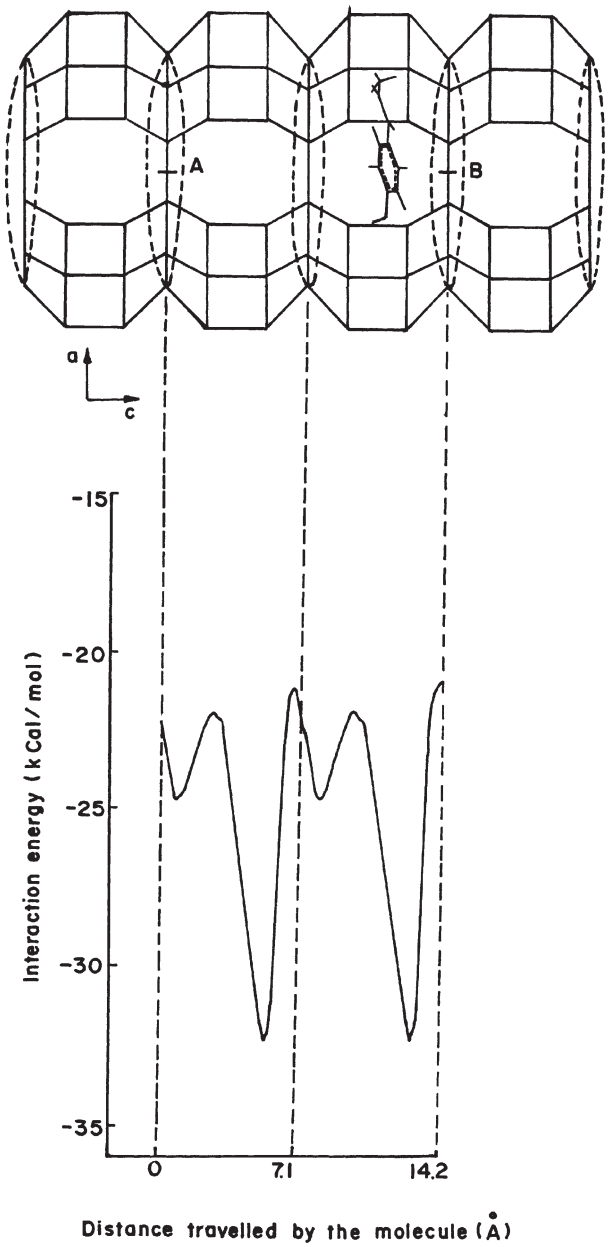

Figure 2. The pore architecture of LTL. The initial and final points (A and B) in the path for the molecules are also indicated. Variation of interaction energy of (**2**) with LTL during diffusion along the c-axis through the barrel-shaped cages is shown. The molecular graphics picture shows a typical minimum energy location for (**2**) in LTL during the diffusion.

reside longer inside the pores due to the specific pore architecture. When the molecules are in a parallel orientation to the c-axis, the largest dimension (a) of the molecules lies along the c-axis. Hence, the second largest dimension (b) is the important parameter to be considered. As can be noted from table 1, the values of (b) for all the molecules are smaller than the diameter of the 12-MR ring (7.1 Å). Again, the diameter of the barrel-shaped cage (12.6 Å) is large enough to fit all the molecules. On this basis, the absence of significant difference in the diffusion energy barrier is rationalized and shape selectivity for molecule (**2**) cannot be expected over LTL.

Table 3
The peak maximum, the deepest minimum and the diffusional energy barriers in kcal/mol for the different molecules in LTL.

Molecule	Peak maximum	Deep minimum	Diffusional energy barrier[a]
1	−15.04	−21.99	6.95 (2.64)
2	−21.98	−32.20	10.22 (4.99)
3	15.69	−31.31	15.62 (5.22)
4	−20.95	−29.58	8.43 (6.03)
5	−19.40	−28.02	8.62 (8.61)

[a] Values in parentheses are diffusion energy barriers calculated assuming that diffusion of the molecules takes place with their largest dimension along the c-direction.

3.2. Diffusion characteristics of molecules in MAZ

Next, we studied the diffusion of the molecules (**1**)–(**5**) in a zeolite with 1-d pores without any cages, namely MAZ. The pores in mazzite formed by 12-MR rings are circular with a diameter of 7.4 Å. Two types of smaller channels are also present; the first is formed by 8-MR rings linking the rows of gmelinite cages and the second is formed by 6-MR rings in the gmelinite cages. As the 6-MR and 8-MR are too small to accommodate any of the molecules (**1**)–(**5**), the diffusion of the molecules along the c-direction in the channel formed by circular 12-MR rings (7.4 Å) is considered. Figure 3 shows the molecular graphics picture of the cross-sectional view of the 12-MR channel. In the c-direction, the unit cell dimension of MAZ is 7.646 Å. The diffusion of the molecules (**1**)–(**5**) in three unit cells along the c-direction was studied and the results of such calculations are shown in table 4. The diffusion energy profile for the molecule (**2**), the desired product, as it diffuses through two unit cells along the 12-MR channel, is shown in figure 3. It is observed that in every unit cell, there is a peak maximum and there are two deep minima. The two minima correspond to the locations where the phenyl rings are present in the stacking points of gmelinite cages shown by arrows in figure 3. In fact, the stacking points lead to small side pockets increasing the diameter of the 12-MR channel by nearly 1.5 Å, thus leading to more space for the molecules. When the phenyl rings cross the 12-MR ring with 7.4 Å diameter, the peak maximum occurs.

The diffusional energy barriers calculated for the molecules in MAZ, as given in table 4, are too small for all the molecules. This is apparently due to the fact that the space available in the zeolite pores is more compared to the size of the molecules. Due to the near absence of energy barriers, MAZ is also not expected to be an efficient shape-selective catalyst.

3.3. Diffusion characteristics of molecules in MOR

Mordenite has an orthorhombic symmetry and a pore structure that is unidimensional. An elliptical 12-MR channel (7.0 Å × 6.5 Å) runs along the c-direction with small pockets (4.7 Å, 8-MR) along the b-direction linking adjacent 12-m channels, these 8-m rings themselves forming a

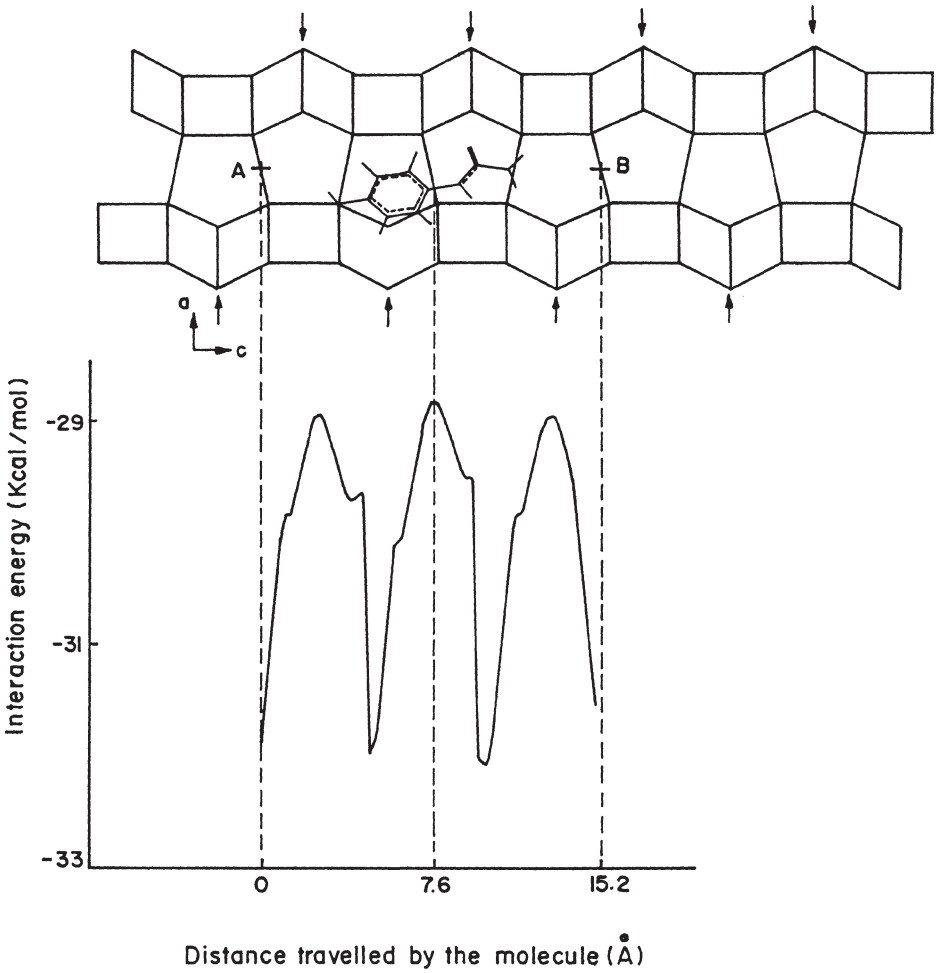

Figure 3. The molecular graphics picture of the cross-sectional view of the 12-MR channel in MAZ. The initial and final points of the diffusion path are also indicated. Variation of interaction energy of (**2**) with MAZ during its diffusion along the c-axis through 12-MR channel is shown. The gmelinite cage stacking points are indicated by arrows. Two such stacking points occur in a single unit cell. A typical minimum energy location for (**2**) in MAZ during diffusion is also shown.

Table 4
The peak maximum, the deepest minimum and the diffusional energy barriers in kcal/mol for the different molecules in MAZ.

Molecule	Peak maximum	Deep minimum	Diffusional energy barrier
1	−22.39	−24.45	2.04
2	−28.64	−32.08	3.44
3	−28.45	−31.45	3.00
4	−28.90	−31.05	2.15
5	−28.09	−30.46	2.37

tortuous channel. Although the 8-m channel is too small for the diffusion of the molecules, the side chains of the aromatic molecules could be accommodated inside the pockets formed by them. The diffusion of all the molecules (**1**)–(**5**) along the c-direction in the 12-MR channel is considered (figure 4). In the c-direction, the unit cell dimension of MOR is 7.524 Å. The diffusion was studied for three unit cells along the c-direction, and the results of the calculation are shown in table 5.

The results in table 5 indicate that there is hardly any barrier for the diffusion of the molecules. Although the diameter of the pore is not large in MOR, the side chains can be located in the 8-MR side pockets. Thus, during the diffusion of the molecules, there are several minimum energy adsorption sites. Due to the tortuous nature of the 8-MR channel along the b-direction, the molecules have a favorable interaction when the phenyl ring of the molecules are in the beginning, end or exact halfway through the 8-m ring. Since the 12-MR channel is elliptical, the favored orientations for all the molecules are those in which the plane of the phenyl ring is parallel to the 8-MR channel opening. The largest dimension (a) of the molecules always lies along the c-direction. We note that the largest dimension of the molecules is the least significant in these single file diffusions. The diffusion of the molecule with the functional groups in the head-side or the tail-side does not make any difference in the diffusion energy profile. However, all these calculations are carried out at zero coverage and the effect of counter diffusion could not be studied. Assuming that the counter diffusion effects will be uniform for all the molecules, no diffusional selectivity could be observed for any of the molecules in MOR.

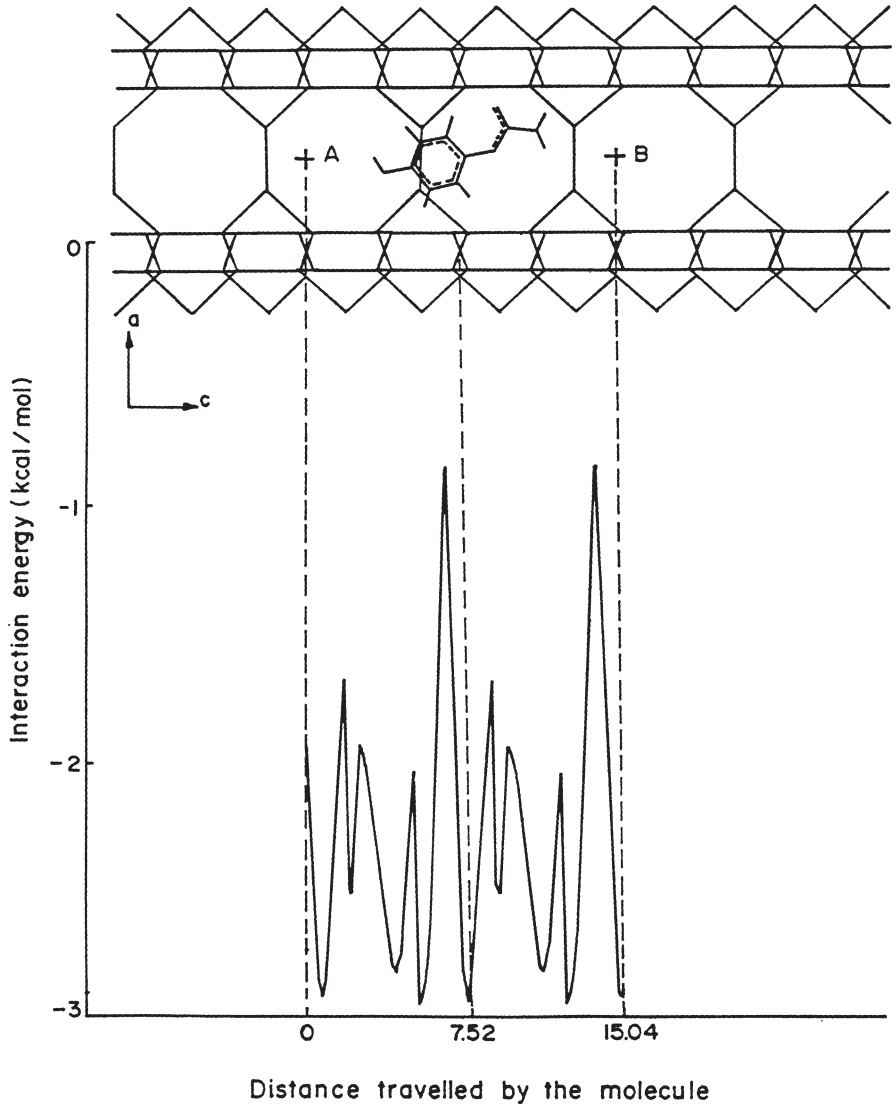

Figure 4. The molecular graphics picture of the cross-sectional view of the 12-MR channel in MOR. The initial and final points (A and B) of the diffusion path are also indicated. The picture also shows 8-MR ring side pockets which link adjacent 12-MR channels. Variation of interaction energy between the molecule (**2**) and the mordenite framework as the molecule diffuses through the 12-MR channel; the interaction energy variation is symmetrically repeated in every unit cell. A typical configuration for the molecule at a minimum energy location is also shown.

Table 5
The peak maximum, the deepest minimum and the diffusional energy barriers in kcal/mol for the different molecules in MOR.

Molecule	Peak maximum	Deep minimum	Diffusional energy barrier
1	−25.18	−26.96	1.78
2	−0.82	−2.93	2.11
3	−33.45	−36.45	2.70
4	−32.94	−34.99	2.05
5	−32.31	−34.69	2.38

3.4. Diffusion characteristics of molecules in MFI

MFI is a medium-pore zeolite with a 10-MR elliptical straight channel along the b-direction. Another circular 10-MR sinusoidal channel runs in the perpendicular direction along the a-direction. The actual dimensions of the pores are given in table 2. However, there are large channel intersections at regular intervals of 4.5 Å. The diffusion of all the molecules (**1**)–(**5**) in the straight channel as well as the diffusion in the sinusoidal channel were simulated following the procedure mentioned earlier. The results of the calculations carried out for the straight channel are given in table 6. The diffusion of the molecules in MFI appears more constrained. In the case of the sinusoidal channels the diffusional energy barriers for all the molecules are higher than in the straight channel, but follow the same order. For example, the reactant (**1**) and the desired product (**2**) have energy barriers of diffusion of 33.08 and 180.52 kcal/mol, respectively. As expected, the interaction energy and the orientations of the molecules at the channel intersections are exactly the same in both cases. These results indicate that the molecules prefer to diffuse through the straight channels rather than the sinusoidal channel. Even the molecules entering the sinusoidal channels are expected to diffuse into the straight channels at the channel intersections.

The interaction energies for the minimum energy configurations for all the molecules are almost the same. However, the C-acylated products have highly unfavorable interaction (maximum energy configuration) with the MFI framework and hence their diffusion energy barrier values are high. Among the N-acylated and O-acylated products ((**2**) and (**3**)), the difference in the diffusion energy barrier is not significant. However, since ZSM-5 is a highly acidic zeolite, the acylation of the acidic phenolic group is not expected to occur. Hence, it appears that MFI will be efficient for the selective production of (**2**) among all the possible products (**2**)–(**5**). Figure 5 shows the molecular graphics picture of the cross-sectional view of the 10-MR straight channel. In this picture, the 10-MR ring openings in the perpendicular direction can also be noticed. However, these 10-MR ring openings are displaced in the alternate layers along the a-direction so that they form a sinusoidal channel. The unit cell dimension along the b-direction for MFI is 19.9 Å; within a unit cell, as shown in figure 5, there are three channel intersections marked as I. The variation of interaction energy of (**2**), as it diffuses in the 10-MR channel along the b-direction, is also shown in figure 5. It could be observed that the molecules have a favorable interaction energy at the three channel intersections (I). On either side of the minima the interaction energy is unfavorable as shown by peak maxima in the diffusion energy profile. This corresponds to the interaction of the molecule with the channel wall. Furthermore, the length of the channel walls,

Table 6
The peak maximum, the deepest minimum and the diffusional energy barriers in kcal/mol for the different molecules in MFI (straight channel).

Molecule	Peak maximum	Deep minimum	Diffusional energy barrier
1	−10.81	−30.06	19.25
2	−16.95	−42.42	25.46
3	−13.59	−41.34	27.75
4	171.09	−44.53	215.63
5	17.58	−37.89	55.47

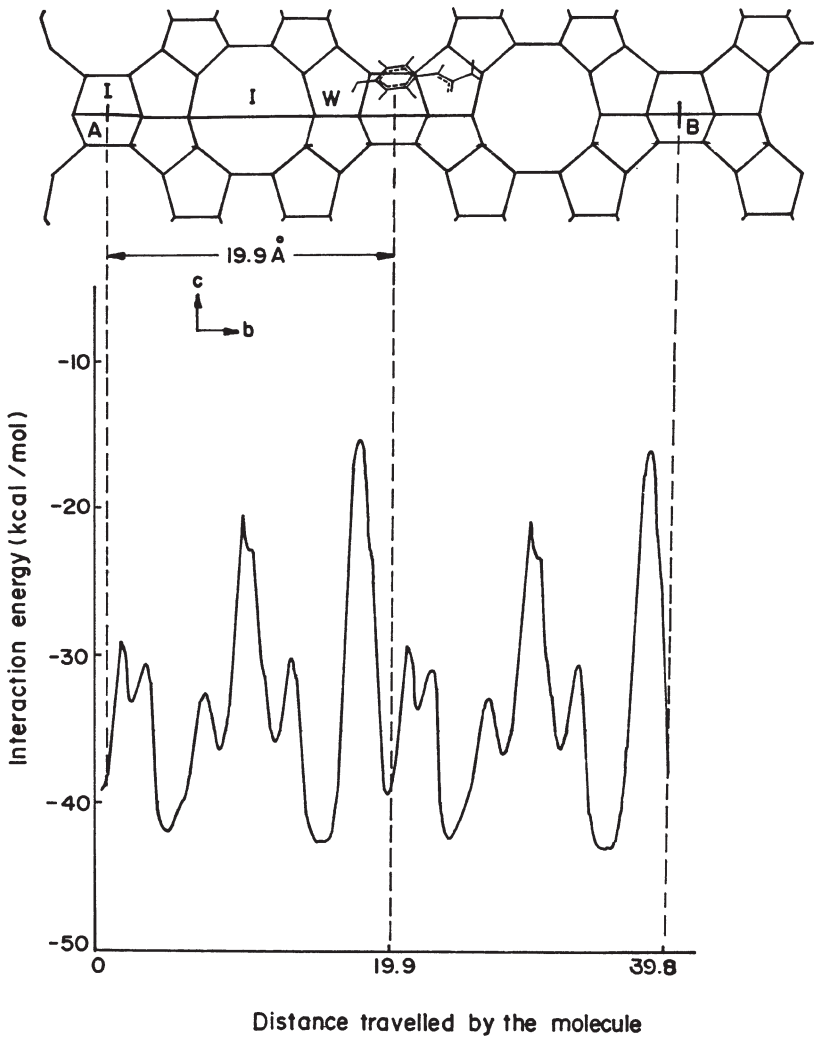

Figure 5. The molecular graphics picture of the cross-sectional view of the 10-MR channel in MFI. The initial and final points (A and B) of the diffusion path are also indicated. A unit cell in b-direction (19.9 Å) has regions of channel intersections (I) and channel walls (W). Variation of interaction energy between the molecule (**2**) and the MFI framework as the molecule diffuses through the 12-MR channel; the interaction energy variation is symmetrically repeated in every unit cell. A typical configuration for the molecule at a minimum energy location is shown.

Table 7
The minimum energy, the mean interaction energy and diffusivity of different molecules in various zeolites.

Molecule	Zeolites							
	LTL		MAZ		MOR		MFI	
	mean	mean/min[a]	mean	mean/min[a]	mean	mean/min[a]	mean	mean/min[a]
1	−16.97	0.77	−22.97	0.94	−25.86	0.96	−23.58	0.78
2	−22.86	0.71	−29.87	0.93	−2.14	0.73	−32.89	0.77
3	−20.70	0.66	−29.97	0.95	−34.70	0.95	−34.21	0.83
4	−24.86	0.84	−29.44	0.95	−33.88	0.97	−29.28	0.66
5	−23.45	0.84	−29.13	0.96	−33.35	0.96	−6.60	0.17

[a] Mean energy/minimum energy ratio is a measure of diffusivity.

marked as W (∼3.0 Å) is much smaller than the length (a) of the molecule (**2**) itself. Hence, the –OH group, the –Ph ring and the –$NHCOCH_3$ group interact individually with the channel wall leading to the splitting of the maxima into triplets. The non-planarity of the 10-rings along the straight channel causes the nonsymmetrical triplet splitting on the left and right maxima. Thus, the heterogeneity in the adsorption sites on the channel walls connecting the channel intersections is brought out by these results.

4. Conclusions

In addition to the diffusion energy barrier, the diffusivity is controlled by the adsorption site heterogeneity in the zeolite pores. During the diffusion, the molecule was allowed to move by 0.2 Å in each step and the interaction energy was calculated. The interaction energy of the molecule with the zeolite framework has been calculated for at least 100 locations along the diffusion path. In addition (considering the difference between the minimum and maximum energy), the mean energy, which is a numerical average of the energy of all locations, was also calculated and given in table 7. The ratio of this mean energy/minimum energy is a parameter which indicates the diffusivity of the molecule. This diffusivity parameter is always in the range of 0–1 and values closer to 1 indicate higher diffusivity. This ratio is also listed in table 7.

We have concentrated only on the influence of pore architecture on the diffusion characteristics of reactants and products. We note that the influence of chemical composition, extraframework cations and the diffusion character of the intermediate will also have to be modeled in the future. The salient conclusions derived from the present study are as follows:

(i) The diffusion energy profiles are extremely sensitive to atomic scale geometry variations in the pore dimensions.

(ii) The diffusion energy barriers for the molecules do not have linear correlation with the dimensions of the molecules. The diffusional energy barrier values are dependent on the structural fitting of the molecules inside the pores.

(iii) In the case of the large-pore zeolites, the channel walls have favorable interaction with the molecules and the windows in the channel lead to unfavorable interaction. By contrast, in medium-pore zeolites, the channel walls have unfavorable interaction.

The results of these calculations predict that the medium-pore zeolite ZSM-5 will show better shape selectivity for the acylation of 4-aminophenol (**1**) to acetanilide (**2**). None of the representative large-pore zeolites analyzed in this study is likely to be a shape-selective catalyst.

Acknowledgement

We thank the Director, NCL for encouragement to carry out this work.

References

[1] H. van Bekkum, A.J. Hoefnagel, M.A. van Koten, E.A. Gunnewegh and A.H.G. Vogt, Stud. Surf. Sci. Catal. 83 (1994) 379.
[2] J.I. Kroschwitz and M.H. Grant, eds., *Kirk-Othmer Encyclopedia of Chemical Technology*, 4th Ed., Vol. 2, p. 597.
[3] T.S. Cantrell, J. Org. Chem. 32 (1967) 1669.
[4] L. Rand and R.J. Dolinski, J. Org. Chem. 31 (1996) 4061.
[5] (a) A.K. Pandey and A.P. Singh, Catal. Lett. 44 (1997) 129;
(b) H.R. Sonawane, A. Sudalai, A.V. Pol and S.S. Biswas, Tetrahedron Lett. 35 (1994) 8897.
[6] P.B. Venuto, Micropor. Mater. 2 (1994) 297.
[7] B. Chiche, A. Finiels, C. Gauthier and P. Geneste, J. Org. Chem. 51 (1986) 2128.
[8] A. Chatterjee and R. Vetrivel, J. Chem. Soc. Faraday Trans. 91 (1995) 4313.
[9] J.A. Horsley, J.D. Fellman, E.G. Derouane and C.M. Freeman, J. Catal. 147 (1994) 231.
[10] Y. Nakazaki, N. Goto and T. Inui, J. Catal. 136 (1992) 142.
[11] R. Millini and S. Rossini, Stud. Surf. Sci. Catal. 105 (1996) 1389.
[12] R.C. Deka and R. Vetrivel, Chem. Commun. (1996) 2397.
[13] A.T. Hagler, S. Lifson and P. Dauber, J. Am. Chem. Soc. 101 (1979) 5122.
[14] P. Dauber-Osguthorpe, V.A. Roberts, D.J. Osguthorpe, J. Wolff, M. Genest and A.T. Hagler, Proteins: Struct. Funct. Genet. 4 (1988) 31.
[15] *Catalysis User Guide*, Version R-4.0 (BioSym Technologies, San Diego, 1993).